Journal scientific and applied research, vol. 6, 2014
Association Scientific and Applied Research
International Journal

Original Contribution

ISSN 1314-6289

SATELLITE MONITORING

Stiliyan Stoyanov, Zhivko Zhekov*

*SPACE RESEARCH AND TECHNOLOGIES INSTITUTE –
BULGARIAN ACADEMY OF SCIENCES
E-mail: stil717@yahoo.com*

**SHUMEN UNIVERSITY "BISHOP KONSTANTIN OF PRESLAV"*
E-mail: zhekov_z@abv.bg

Abstract. *In the current paper, satellite methods for research of gas content of the atmosphere are presented. The stress is on the satellite methods and the measurement geometry. A generalized characteristic of the absorption specters of the atmospheric ozone and gases into the optic range is presented when research with land and satellite appliances and apparatuses.*

An evaluation of the satellite methods is made when measuring the content of small gases.

Scientific results are presented which are received by satellite experiments and the perspectives of satellite research are laid down.

Key words: *satellite methods, gas content of the atmosphere*

Study of the gas composition of the atmosphere through various methods is carried out for many decades. The interest in this problem significantly increased in recent years due to the following main reasons:

- the significant increase of content of gases and aerosols with anthropogenic origin in atmospheric composition;
- better understanding of the various physical mechanisms affecting the change of the gas and aerosol composition of the atmosphere, the different characteristics of the environment and in particular the weather and Earth's climate.

Earlier the attention were focused on the rise of carbon dioxide concentration (CO_2), but today estimates are that the concentrations of some other trace gaseous components (TGC) as CH_4, CO, N_2O, CFCs and etc. in the

near future could possibly affect the Earth's climate more substantially than the rise of CO_2 concentration solely.

The change in the gas composition and its potential impact on the climate stimulate creation and functioning of various systems for monitoring of gas composition of the Earth's atmosphere. Systems located on the Earth's surface measure changes in the content of O_3, CO_2, H_2O and many other TGC. Still more attention is paid to the airplane and aerostatic measuring of the TGC. Derived in this manner data constitute a large amount of important information about the spatial - temporal variations in the content of the TGC and about the intensity of their sources.

A significant contribution to obtaining such information have the satellite measurement methods [3, 4, 7, 11 ... 14]. Their role in the future will undoubtedly increase, which is due to the possibility of getting global uniform three-dimensional information about the content of many TGC with good frequency for long period of time.

SATELLITE METHODS AND GEOMETRY OF THE MEASUREMENTS

For the study of the gas composition of the atmosphere, three satellite passive methods are subject of intensive use (Fig. 1).

- Method of transparency (TRA) in which information about the content of the TGC is derived from the solar radiation absorption spectra on the appearance and setting of the sun behind the horizon of planets (possible use of the moon and stars);
- Method of thermal radiation (TR) using the measurements of the spectral and (or) the angular dependence of the atmospheric own radiation;
- Method of reflected and scattered solar radiation (RSSR), in which information about the content of the TGC is derived from measuring the radiation in the ultraviolet (UV), visible (VIS) and near-infrared (NI) region of the spectrum.

In the recent years we observe development of various laser methods for probing of the atmosphere, including the characteristics of its gas composition. Laser experiments are under planning and preparation. Significant amount of information about the content of the TGC in the Earth's atmosphere will be obtained by the above - mentioned three passive satellite methods.

The satellite measurements of TGC use two types of measurement geometries: nadir and tangential (to the horizon of the planets), substantially differing in spatial resolution.

While with tangent geometry can be achieved relatively high vertical resolution (1 ... 4 km depending on the angular aperture of the satellite device), resulting with the average experimental characteristics of the composition of the

atmosphere (300 ... 500 km and more), at nadir measurements the situation is reversed: the vertical resolution is 8 ... 10 km and better, and the horizontal can reach approximately 10 km. The height (upper limit) of probe at distant methods is determined by the sensitivity of optical devices, the optical density in specific areas of absorption and the geometry of measurement.

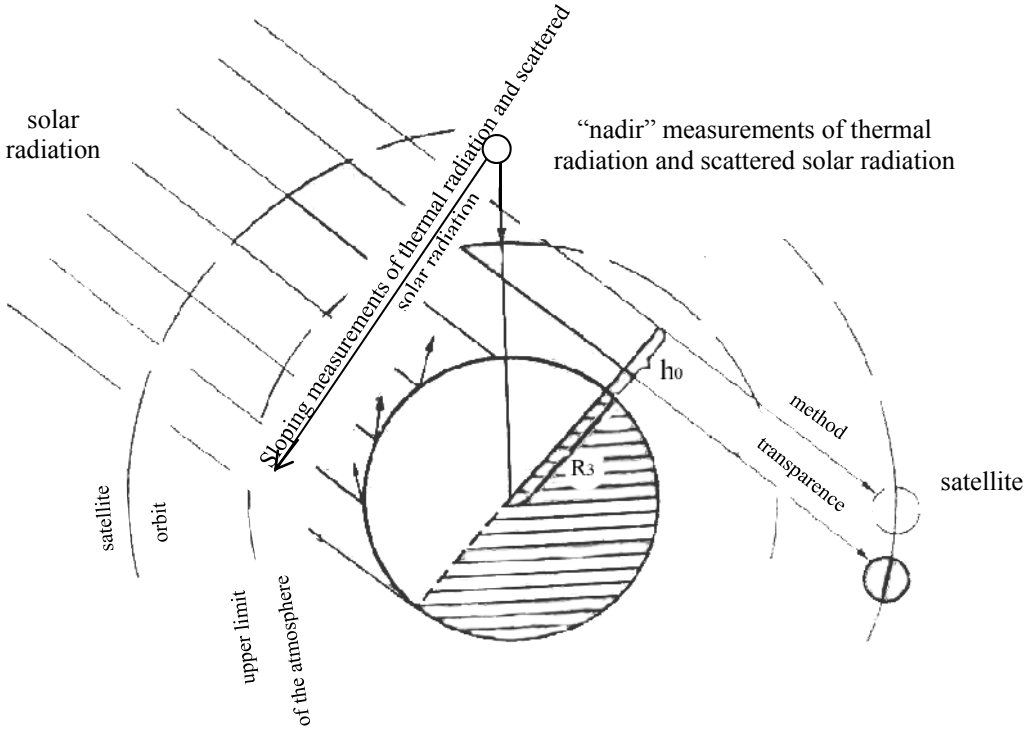

Fig. 1. Satellite passive methods and geometry of measurements of TGC (h_0 - informative height, R_3 - the radius of the Earth)

In this regard, almost all modern indirect methods in the thermal region of the spectrum are based on the assumption of local thermodynamic equilibrium (LTE).

Frequency of measurements (number of measurements in days) varies depending on the different methods and is determined by the orbits of the satellites, the operating modes of satellite equipment and the geometry of measurement. For TRA method the number of measurements per day is around 30 when using the Sun as a source, and can reach 103 ... 104 with methods TR and RSSR. The level of global coverage of the Earth's expanse by satellite observations is determined by the method, the characteristics of the orbit, the geometry of the observation, the characteristics of satellite equipment and the operating modes. TR methods are characterized with greatest information capacity and TRA method with use of only solar radiation is characterized with the poorest. A comparative analysis of the indirect methods show that various

methods have their advantages and disadvantages. In this connection it is important to create the optimum combination for launching of a global system for monitoring of the TGC consisting of land, air, aerostatic and satellite measurements.

In all the above mentioned areas, the effectiveness of scientific research is inextricably linked to the creation of tools and instruments for conducting measurements with high accuracy. Among the various types of modern measuring instruments, the top positions belong to the optical, electron - optical and opto-electronic devices and equipment.

STUDY OF THE REMOTE OBJECTS VISIBILITY WITH VIEWFINDERS OPTICAL DEVICES AT VARIOUS BACKGROUND BRIGHTNESS

The suggested methodology provides a full scale of characteristics of the studied distant objects based on the brightness of the background against which they are tested, determined by the effectiveness N_0 at the center of the field of vision of the peep-sight, at determining the marginal illumination at the center of the visual field, at different field angles β, when determining the shape coefficient and the diameter of the aberration spot ρ, by determining the effectiveness $N_{\rho,\beta}$ and by taking into account the influence of aberration scattering and field angle and determination of marginal illumination in the image plane accounting for the above factors, in terms of highlighting of the peep-sight optical system by the Sun, Moon and planets.

1. Determining the coefficient K_d reflecting the partial use of the area of the pupil of the eye:

(1) $$K_d = d/\delta,$$

where: d – diameter of the instrument's exit pupil;
δ – diameter of the pupil of the observer's eye.

The size of the pupil diameter is determined depending on the brightness of the background. If the diameter of the eye pupil $d \geq \delta$, than the coefficient K_d shall be considered equal to 1.

1. Calculation of the coefficient K_δ reflectring the Stiles-Crawford effect, which characterizes the ratio of the aggregate effect of light passing through the exit pupil of the instrument with diameter $d = 2x_1$ to the aggregate effect of light on the observer's eye pupil with a diameter $\delta = 2x_2$, which vary in dependence to the background brightness:

(2) $$K_\delta = Sx_1/Sx_2,$$

where: $x_1 = d/2$, a $x_2 = \delta/2$.

3. Measuring of the effectiveness N_0 in the center of the visual field of the viewfinder according to the equation:

$$N_0 = \Gamma^2 (K_d^2 \tau_{o.s.} \tau_{atm})^{1-n}, \quad (3)$$

where: τ_{atm} – coefficient of light transmittance of the atmosphere;

$\tau_{o.s.}$ – coefficient of light transmittance of the optical system of the device:

$$\tau_{o.s.} = 0{,}99^{l_{sm}} 0{,}95^{N_{cr}} 0{,}94^{N_{fl}}, \quad (4)$$

where: $N_{cr} N_{fl.}$ – number of crown and flint optical elements with no adhesive;

l_{sm} – total length of all the optical elements in the system;

n – exponent, which reflects the influence of the background brightness.

4. Definition of marginal illumination E_0 in the center of the visual field according to the equation:

$$E_0 = E_N / N_0, \quad (5)$$

where: E_N – observed marginal illumination with the naked eye

$$E_N = cB^n, \quad (6)$$

the value of E_N is determined depending on the brightness of the background B.

5. Measuring the effectiveness N_β for field angles β_i according to the equation :

$$N_0 = \Gamma^2 (K_d^2 K_\delta \tau_{o.s.} \tau_{atm})^{1-n} \cos\beta, \quad (7)$$

where: $K_\beta = K_d^2 K_\delta \alpha_\beta$

α_β – vignette value in field corners β ;

6. Definition of the form coefficient of the aberration spot at the ratio *l/h* – length to width of the rectangular aberration field.

$$q = E_{l,h} / E_\rho. \quad (8)$$

7. Calculation of the diameter of the aberration circle according to the equation:

$$\rho = \sqrt{lh/\pi}. \quad (9)$$

8. Definition of marginal illumination of the object in the image plane E'_ρ using the calculated ρ .

9. Definition of effectiveness $N_{\rho,\beta}$ of the accounting of the impact of the aberration scattering spot in the viewfinder and field angle β.

(10) $$N_{\rho,\beta} = N_\beta E_H / E'_\rho q .$$

10. Definition of marginal illumination $E_{\rho,\beta}$ considering the influence of aberration scattering spot in the viewfinder and field angle β.

(11) $$E_{\rho,\beta} = E_H / N_{\rho,\beta} .$$

11. When the researched elongated object has wide spectrum under the marginal illumination $E_{\rho,\beta}$ a coefficient $E_{\rho,\beta}$ is introduced to define $E_{col.}$

(12) $$E_{col.} = E_{\rho,\beta} P_{col.}$$

In determining the visibility of distant point objects studied in case of illumination by the Sun or planets, it is necessary to know the illumination of the optical parts by the Sun E_s, the angle of the lateral illumination of the viewfinder optical system α_s or respectivly by the planets, the background brightness B_{pl} by the planets, the angle of lateral illumination α_{pl} and angular dimension of the illuminating source L (or the solid angle of the illuminating source).

For this purpose:

1. Calculation of the illumination of the planets on the inlet of the viewfinder:

(13) $$E_{pl} = B_{pl} w.\cos\alpha ,$$

where $\alpha = 2\pi(1 - \cos L/2)$.

2. Calculation of the brightness coefficient r_α of the viewfinder protective glass and other optical components, illuminated by the planets or the sun at angle α .

3. Definition of the brightness of scattered light background in a lateral illumination from the sun B_s or planets B_{pl} .

(14) $$B_{s,pl} = \frac{E_{s,pl}.r_\alpha}{\pi} ,$$

where $E_s = E_\perp \cos\alpha$

$E_\perp = 13{,}5.10^4 lk$ for the atmosphere.

VIEWFINDER OPTICAL DEVICES

In determining the light balance of visual optical and electron- optical devices for monitoring of remote objects from the orbiting space stations, taking into account the effects of different optical characteristics of the device, the brightness of the background against which the observations are carried out , the influence of aberration spot scattering, the parameters of the scale, theoretical and experimental research was carried out and are designed “Vizir B 3x40” for observation of remote objects as part of the photometric equipment “Rainbow” and Vizir – target 15 K for remote monitoring with the spectrozonal equipment “Spectrum 15K”.

Vizir – target 15 K

Spectrozonal equipment “Spectrar 15 K” consist of two main sections. The first section constitutes an optical mechanical structure designed to targeting and optical processing of the researched data signal, and then transmit the signal to the recording unit, which is designed to evaluate the signal, to strobe and convert it into digital indication and to perform recording on magnetic tape.

Targeting of the equipment is provided by "Vizir - target 15 K" (Fig. 3), representing a viewfinder optical system (Fig. 2) with the following optical characteristics:

1. Magnification of viewfinder-target – $3{,}16^{x}$
2. Visual field – 14º
3. Diameter of the inlet opening – 18 mm.
4. Diameter of the exit pupil – 5 mm.
5. Distance of the exit pupil – 26,7 mm.
6. Resolution – 19´´
7. Marginal locked focus of eyepiece for sharpness of the image ± 4 diopters
8. Value of the smallest division of the grid:

- horizontal - 1º
- vertical - 1º

9. Capacity for signal pass $\tau = 0{,}52$
10. Geometric vignetting $\alpha_{\beta} = 1{,}0$
11. Size of the spot of scattering $lh = 11'2'$

Photometric calculation according to the proposed methodology is presented in Table 1.

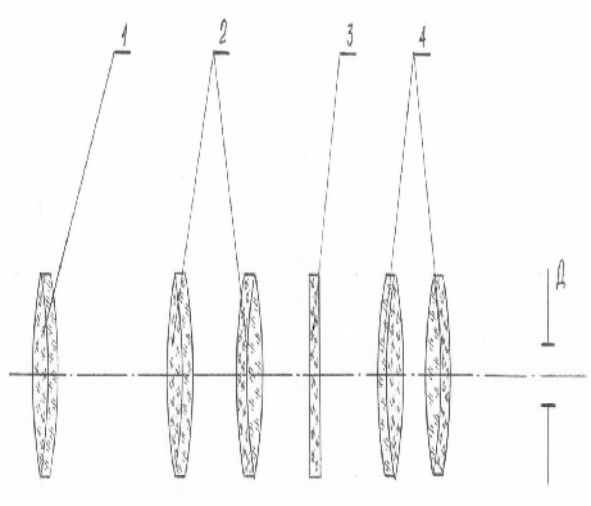

Fig. 2. Optical system of "Vizir – target 15 K"

Fig. 3. Vizir – target 15 K

Table 1. Photometric characteristics of Vizir target 15 K

№	Characteristics	Background brightness B [kd/m^2]			
		$B \le 10^{-4}$	$10^{-4} < B < 0{,}05$	$0{,}05 < B < 20$	$20 < B < 4200$
1	K_d	5/7	5/6	1	1
2	K_δ	1,3	1,14	0,9	0,8
3	N_0	3,45	6,2	7,77	8,68
4	$E_н$, lk	10^{-8}	10^{-7}	10^{-6}	10^{-5}
5	E_0, lk	$2{,}9.10^{-10}$	$1{,}61.10^{-9}$	$1{,}29.10^{-8}$	$1{,}61.10^{-7}$
6	N_β	3,4	5,934	7,66	8,46
7	q	1,33	1,33	1,33	1,33
8	ρ	2,7	2,7	2,7	2,7
9	E_ρ	10^{-9}	10^{-8}	10^{-7}	10^{-6}
10	$N_{\rho,\beta}$	2,56	4,464	5,763	6,361
11	$E_{\rho,\beta}$	$3{,}91.10^{-9}$	$2{,}24.10^{-8}$	$1{,}74.10^{-7}$	$1{,}57.10^{-6}$
12	P_{red}	39	39	20	2,2
13	E_{red}	$1{,}525.10^{-8}$	$8{,}74.10^{-8}$	$3{,}47.10^{-7}$	$3{,}46.10^{-6}$
14	P_{green}	48	48	24	3
15	E_{green}	$1{,}877.10^{-8}$	$1{,}08.10^{-7}$	$4{,}16.10^{-7}$	$4{,}72.10^{-6}$

Optical viewfinder Vizir B 3x40

Equipment "Rainbow" consists of two main blocks. First one called OM (Optical-mechanical) is an opto-mechanical structure whose task is to guide through the viewfinder system the electrical photometer to analyze the monitoring of the atmosphere.

Vizir B 3x40 (fig. 6), with optical system as shown in Figure 5, has the following technical characteristics:

1. Magnification of the viewfinder – $2,6^{x}$
2. Visual field – 23º
3. Diameter of the inlet opening – 40 mm.
4. Diameter of the exit pupil – 6 mm.
5. Distance of the exit pupil – 22,5 mm.
6. Resolution – 23”
7. Marginal locked focus of eyepiece for sharpness of the image ± 4 dptr.
8. Value of the smallest division of the grid:
   - horizontal -1º30
   - vertical - 1º30
9. Total length of the viewfinder – 380 mm.
10. Weight of the viewfinder – 0,850 kg.

Photometric values are presented in Table 2.

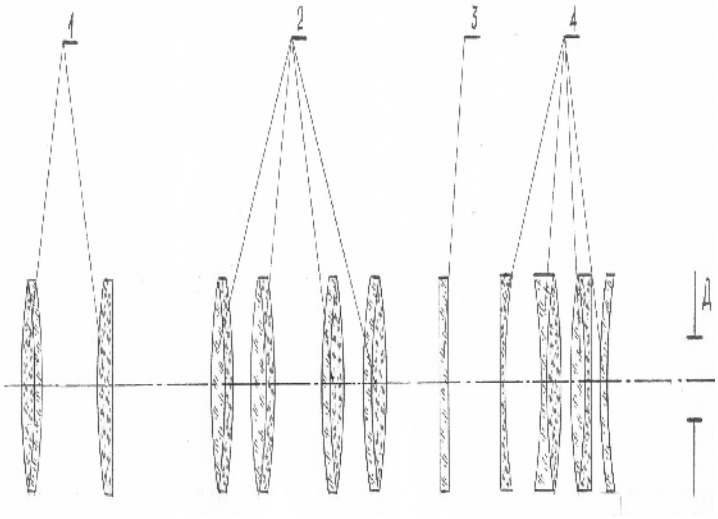

Fig. 4. Optical system of Vizir B3x40

Fig. 5. Vizir B 3x40

Table 2. Photometric characteristics of Vizir B3x40

№	Characteristics	Background brightness B [kd/m^2]			
		B≤10^{-4}	10^{-4}<B<0,05	0,05<B<20	20<B<4200
1	K_d	5/7	1	1	1
2	K_δ	1,3	1	0,8	0,7
3	N_0	2,18	3,94	4,39	5,34
4	$E_н$, lk	10^{-8}	10^{-7}	10^{-6}	10^{-5}
5	E_0, lk	$4{,}59.10^{-10}$	$2{,}54.10^{-9}$	$2{,}28.10^{-8}$	$1{,}87.10^{-7}$
6	N_β	2,94	3,88	4,33	5,26
7	q	1,27	1,27	1,27	1,27
8	ρ	17	17	17	17
9	E_ρ	10^{-9}	10^{-8}	10^{-7}	10^{-6}
10	$N_{\rho,\beta}$	2,31	3,06	3,41	4,14
11	$E_{\rho,\beta}$	$4{,}33.10^{-9}$	$2{,}27.10^{-8}$	$2{,}93.10^{-7}$	$2{,}42.10^{-6}$
12	P_{red}	39	39	20	2,2
13	E_{red}	$1{,}68.10^{-8}$	$1{,}28.10^{-8}$	$5{,}86.10^{-7}$	$5{,}32.10^{-6}$
14	P_{green}	48	48	24	3
15	E_{green}	$2{,}08.10^{-8}$	$1{,}56.10^{-7}$	$7{,}03.10^{-7}$	$7{,}26.10^{-6}$

Fig. 6. Zoom viewfinder Vizir 8 – 20x50

Table 3. Photometric characteristics of Vizir 8 – 20x50

№	Characteristics	Background brightness B [kd/m^2]			
		$B \leq 10^{-4}$	$10^{-4} < B < 0{,}05$	$0{,}05 < B < 20$	$20 < B < 4200$
1	K_d	5/7	1	1	1
2	K_δ	1,34	1,22	1	0,9
3	N_0	3,49	6,31	7,04	8,54
4	$E_н$, lk	10^{-8}	10^{-7}	10^{-6}	10^{-5}
5	E_0, lk	$3{,}77.10^{-10}$	$2{,}09.10^{-9}$	$1{,}68.10^{-8}$	$2{,}09.10^{-7}$
6	N_β	3,82	5,04	5,63	6,84
7	q	1,31	1,31	1,31	1,31
8	ρ	4,3	4,3	4,3	4,3
9	E_ρ	10^{-9}	10^{-8}	10^{-7}	10^{-6}
10	$N_{\rho,\beta}$	2,46	3,36	3,75	4,55
11	$E_{\rho,\beta}$	$4{,}30.10^{-9}$	$2{,}46.10^{-8}$	$1{,}91.10^{-7}$	$1{,}73.10^{-6}$
12	P_{red}	39	39	20	2,2
13	E_{red}	$1{,}59.10^{-8}$	$1{,}76.10^{-8}$	$6{,}15.10^{-7}$	$5{,}84.10^{-6}$
14	P_{green}	48	48	24	3
15	E_{green}	$2{,}29.10^{-8}$	$1{,}72.10^{-7}$	$7{,}73.10^{-7}$	$7{,}98.10^{-6}$

PHOTOMETRIC DEFINITION OF EFFECTIVENESS OF ELECTRONIC OPTICAL DEVICES FOR MONITORING OF THE ATMOSPHERE

The essence of the method is to study the marginal sensitivity at certain parameters. Value that characterizes the sensitivity of the device is represented by the marginal energetic illumination of inlet orifice by the signal/noise ratio or by the limit value of the flow emitted from the object at a certain level of noise.

The methodology of the energetic study of electron optical viewfinders has significant specificities compared to that of optical and opto-electronic devices. Since electron optical instrument consists of optical, photoelectronic, electrotechnical and luminescent devices, when determining the parameters it is necessary to apply different methods of research and coordination of the characteristics of these devices. For each of the methods it is necessary to take into account the size and nature of the required information regarding the researched object, allowing to detect the object and to determine its limits or to provide a detailed study of its structure. Depending on these conditions changes not just the range of the tested objects, but the sequence of stages of power calculations [1 ... 3].

Upon detection of remote objects, it is necessary to specify the following conditions:

- marginal contrast brightness of the observer's pupil of the eye;
- light-technical characteristics of the surveyed object;
- taking into account the impact of the atmosphere;
- examination of marginal illumination of the photocathode by alleged irradiance of the object and its background;
- comparing the results with marginal contrast sensitivity of the eye at specified observation conditions.

In order to determine the effectiveness of electron optical instruments a methodology is proposed, developed on the basis of theoretical research and experiments conducted by the author, which provides study of the possibility of detecting remote objects in an environment of varying brightness of the background.

1. Calculation of the effective energetic illumination of the image on the photocathode $E_{ef\,fk}$:

(15)
$$E_{ef\,fk} = \frac{A_{il}}{n\Gamma^2 L^2} \int_{\lambda_0}^{\lambda_k} (\sqrt{\lambda} + \rho_\lambda e_\lambda) \tau_{\lambda_f} \tau_{\lambda_{op}} \tau_{\lambda_{atm}} d\lambda ,$$

where: A_{il} – area of the inlet lens;

Γ – magnification of the optical system;

e_λ – energetic illumination of the inlet;

L – observation distance;
$\lambda_0..\lambda\kappa$ – spectral range of the research;
ρ_λ – spectral coefficient of the reflected filters;
τ_{λ_f} – spectral transmittance of the applied filters;
$\tau_{\lambda_{op}}$ – spectral transmittance of the optical system;
$\tau_{\lambda_{atm}}$ – spectral transmittance of the atmosphere.

2. Calculation of impact of external noise fluctuations on the image brightness by the coefficient determining the image contrast:

(16) $$K_{sch_i} = \frac{1}{2N_{fk}}\sqrt{\frac{t}{2\lambda}S_{\lambda_{\max}}E_{ef_{fk}}},$$

where: N_{fk} – quantum output of the the photocathode;
t – the time of the experiment;
S_λ – spectral sensitivity of the the photocathode.

3. Determination of the coefficient that characterizes the signal/noise ratio for the dark current K_{sch_t}:

(17) $$K_{sch_t} = \frac{E_{ef_{fk}}S_{\lambda_{\max}}}{J_t},$$

where: J_t – dark current at the photocathode;
$S_{\lambda_{\max}}$ – maximum spectral sensitivity of the photocathode.

4. Calculation of the signal/noise ratio at measuring of the noise which results from the information signal implification by the electronic-optical converter and the dark current:

(18) $$K_{sch} = \frac{E_{ef_{fk}}S_{\lambda_{\max}}\sqrt{t}}{\sqrt{4e_\lambda N_{fk}^2 E_{ef_{fk}}S_{\lambda_{\max}} + J_t^2}}.$$

5. Calculation of the background brightness on the exit of electron optical viewfinder:

(19) $$B' = K_{sch}\left(\frac{\tau_{\lambda_{op}}K_d^2 K_b}{4\Gamma_{EOP}^2}\right)\left(\frac{D}{f'_{ob}}\right)$$

where: K_d – coefficient accounting for the Stiles-Crawford effect;
K_b – coefficient accounting for the impact of the pupil of the eye;
Γ_{EOP} – optical zoom of the electronic - optical converter;
D – diameter of the inlet;
f' – back focal length of the lens.

6. Defining of the diameter of the observer pupil of the eye and the coefficients K_d and K_b for B'.
7. Calculation of the exponent n and n' respectively for B and B'.
8. Calculation of the effective illumination $E_{ef\,fk}$ of the object on the photocathode:

(20)
$$E_{ef\,fk} = \frac{2e_{\lambda} N_{fk}^2 K_{sch} + K_{sch}\sqrt{4e^2 N_{fk}^4 + J_t^2 t}}{tS_{\lambda_{\max}}}.$$

9. Calculation of the effective illumination of the background image on the photocathode:

(21)
$$E_{ef\,fk\ fon} = \frac{A_{ob} R_{ef}}{nA_{fk}},$$

where: R_{ef} – energetic illumination of the object;
A_{fk} – area of the photocathode of the electronic-optical converter.

10. Determining the image contrast K:

(22)
$$K = \frac{E_{ef\,fk_{ob}} + E_{ef\,fk\,fon}}{E_{ef\,fk_{ob}} - E_{ef\,fk\,fon}}.$$

11. Determining of the marginal image contrast K':

(23)
$$K' = \frac{1+K}{1-K}.$$

12. Determining of the effectiveness N_{EOV} of electron optical viewfinder:

(24)
$$N_{EOV} = \frac{K' A_{ob} (D^2 t K_d^2 K_b)^{1-n'} (\Gamma_{EOP}\, f'_{ob})^{2n'}}{o{,}25^n 4 (f'_{ob})^2},$$

where: n – exponent that characterizes the influence of the background brightness.

13. Calculation of the marginal illumination of the viewfinder:

(25)
$$E_{EOV} = E_H / N_{OEV},$$

where: E_H – marginal illumination observed with naked eye.

Using the proposed methodology were conducted experimental studies of electron optical instruments – Figure 7 and Figure 8 and Table 3 shows results of an exemplary application of an electronic-optical device Parallax represented on the Figure 7.

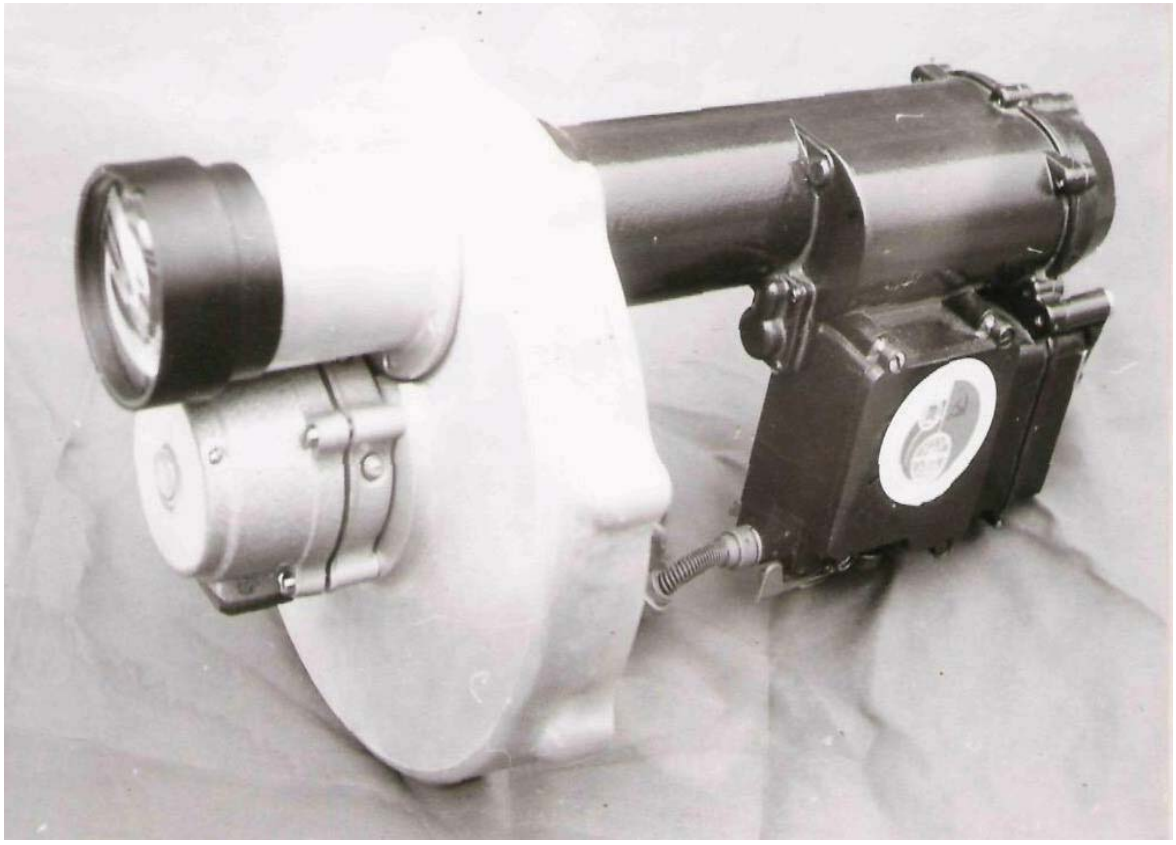

Fig. 7. Electron optical viewfinder for testing of particular atmospheric emissions in the near infrared part of the optical spectrum

Fig. 8. Electron-optical instrument Parallax

Table 3. Photometric characteristics of electron-optical instrument Parallax

№	Characteristics	Background brightness [cd/m^2]	
		$B = 1.10^{-5}$	$B = 1.10^{-3}$
1	$E_{ef\ fk}$	5,88	5,88
2	K_{sch_i}	0,12	0,12
3	K_{sch_t}	0,02	0,04
4	K_{sch}	0,19	0,19
5	B'	$7{,}7.10^{-6}$	$7{,}8.10^{-2}$
6	K_d	1	1
7	K_b	1	1
8	n	0	0,24
9	n'	0	0,53
10	E_H	10^{-8}	10^{-7}
11	K'	1,45	1,56
12	N_{OEV}	44	44
13	E_{EOV}	$2{,}75.10^{-11}$	$4{,}07.10^{-9}$

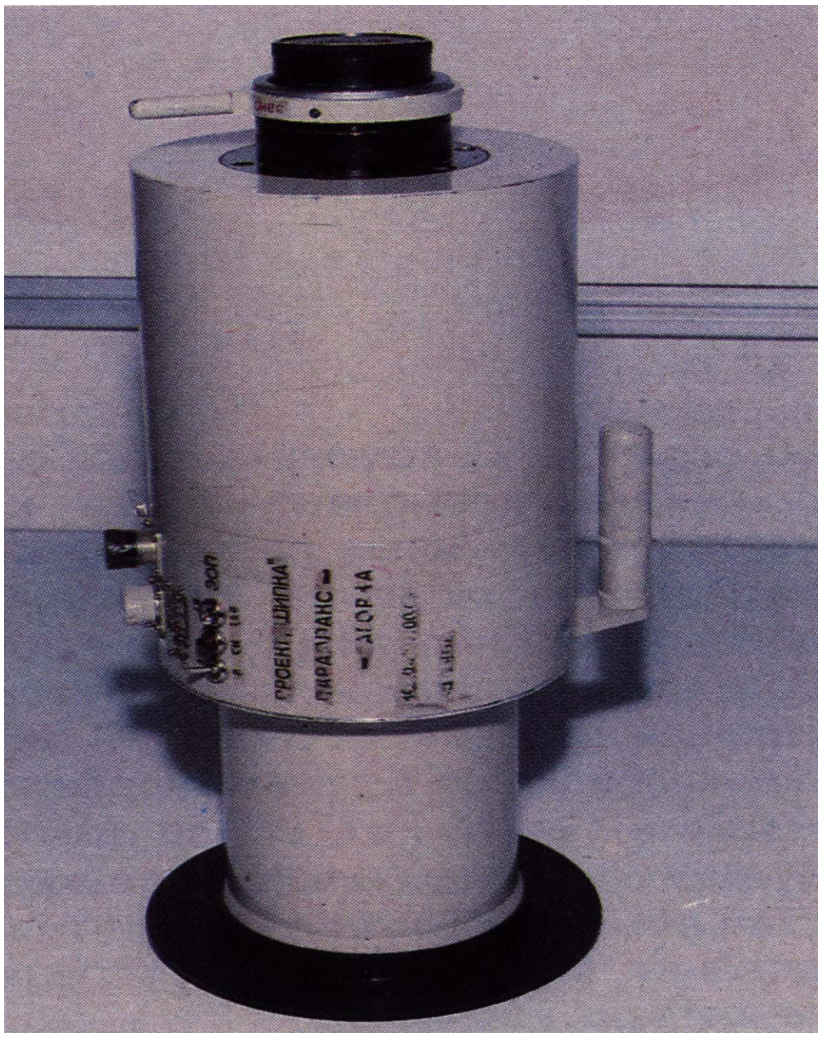

Fig. 9. Parallax Zagorka

METHODS AND MEANS FOR MONITORING OF THE ATMOSPHERE THROUGH OPTICAL-ELECTRONIC DEVICES

IMPULSE PHOTOMETRIC EQUIPMENT "THERMA"

The necessity of conducting research at orbital stations and by sub-satellite measurements required the development of a wide range of scientific research equipment.

Impulse photometric equipment "Therma" is designed for high spatial and temporal resolution research of the distribution of the intensity of natural optical emissions in the Earth's atmosphere and light disturbances in the vicinity of the orbital station "Mir". High spectral sensitivity and spatial resolution allows the study of rapidly changing areas of light as occultation stars, lightning activity, pulsating auroras, polar arcs and others.

Information from impulse photometric equipment "Terma" (fig. 24) in the form of a stream of photons is converted, formed and transmitted through

electronic - digital block to the on-board system for data collecting and processing “Zora”.

Fig. 10. External view of impulse photometric equipment “Terma”

Technical characteristics
Spectral range of the integral channel: 200-630 nm.
Number of narrowband spectral channels 4.
Average width of the photometric channel 2,5±1 nm at level 0,5.
Main lens - diverging lens with inlet 82 mm.
Field of view (angular): 15 ', 30', 1°, 2°.
Angular field of view of the viewfinder 23°.
Viewfinder magnification 2.6^{x}
Sensitivity threshold of the equipment without interference filters - 10R (relay) at a wavelength of 600 nm.
Transmission coefficient of interference filters: $\tau = 30\%$
Temporal constant: 10^{-4} s.
Dynamic range of measuring with the equipment: 2.10^{5}.
Range of targeting the equipment in the carrier ±8°.
Torque of the device into the carrier 100 g/sm.

Power consumption ≤ 30Wt
Weight of the equipment without container 8 kg
Weight of the container 5 kg
Weight of the individual reservists accessories 1 kg
Overall dimensions of the equipment 540 x 315 x 315 mm.

Operating mode of the equipment: optional speed of information recording, optional sensitivity, aperture size, time for measurement and position the equipment.

Optimal mode is possible only if there is a priori information about the surveyed heterogeneity. Unlike quantitative measurements, qualitative measurements show the dynamics of change and the properties of the target object. This necessitates more detailed examination of the characteristics of application and use of photometric methods.

The brightness of a specific point in the image plane of optical-electronic tract, in the absence of heterogeneity is determined by the expression:

(26)
$$E(x,y) = \int_{-\sim}^{\sim}\int_{-\sim}^{\sim} E(x,y,\xi,\eta)\tau(\xi,\eta)d\xi d\eta\ ,$$

where:
- (x,y) – coordinates in the image plane;
- (ξ,η) – coordinates in the plane of the diaphragm;
- $\tau(\xi,\eta)$ – Translucence through the diaphragm depending on the settings;
- $E(x,y,\xi,\eta)$ – value of the luminous flux at a point on the the image plane with coordinates (x,y).

Researched heterogeneity diverges light rays and changes the image formed by rays passing through each point of granularity. Brightness at that point of the image $E^{|}(x,y)$ will be equal to:

(27)
$$E^{|}(x,y) = \int_{-\sim}^{\sim}\int_{-\sim}^{\sim} E\{x, y[\xi + \varepsilon f\cos\alpha][\eta + \varepsilon f\sin\alpha]\}\tau(\xi,\eta)d\xi d\eta,$$

where:
- ε – angle of deflection of the light rays at a point of the heterorogeneity in the corresponding image region with coordinates (x,y);
- α – angle defining the direction of deflection of the light beam from the same point of heterorogeneity;
- f – focal length of the photometric part.

If the function $E^{|}(x,y)$ changes smoothly with the variation of ξ and ηthen at small angles of deflection of the light rays the sensitivity G can be represented as follow:

(28)
$$G=\frac{dE^{|}}{Ed\varepsilon}=\frac{f\int\limits_{\sim\sim\sim\sim}^{\sim}\int\limits^{\sim}\left[\frac{dE}{d\xi}\cos\alpha+\frac{dE}{d\eta}\sin\alpha\right]\tau(\xi,\eta)d\xi d\eta}{\int\limits_{\sim\sim\sim\sim}^{\sim}\int\limits^{\sim}E(x,y,\xi,\eta)\tau(\xi,\eta)d\xi d\eta},$$

(29)
$$G=G_{\xi}\cos\alpha+G_{i}\sin\alpha,$$

where: G_{ξ},G_{η} - measurements sensitivity at deflection of light rays relative to the axes ξ and η.

For convenience expression (29) can be represented in the form:

(30)
$$G=G_{\xi}\left(\cos\alpha+\frac{G_{\eta}}{G_{\xi}}\sin\alpha\right).$$

As a result of the heterorogeneity arises further shift of the light source image in a direction which is characterized by the angle β .

Illumination of an image point without a heterogeneity is equal to:

(31)
$$E=\delta_0 h_a,$$

where: h_a - size of the projection of the illuminated part of the plane (ξ,η) in a direction perpendicular to the vector of displacement of the image of the light source relative to the diaphragm.

In the presence of heterogeneity, the image illumination $E^{|}$ changes and becomes:

(32)
$$E^{|}=\delta^{|}h_{\gamma},$$

where:

(33)
$$\delta^{|}=\sqrt{\varepsilon^2 f^2+\delta^2+2\varepsilon f\delta_0\cos(\alpha-\beta)},$$

(34)
$$h_{\gamma}=\alpha+ar\cos\frac{\delta_0+\varepsilon f\cos(\alpha-\beta)}{\sqrt{\varepsilon^2 f^2+\delta_0^2+2\varepsilon f\delta_0\cos(\alpha-\beta)}}.$$

The sensitivity of measurement when $\varepsilon\to 0$ is equal to:

(35)
$$G=\frac{f}{\delta_0}\left[\cos(\alpha-\beta)-\frac{dh_a}{d\alpha}.\frac{\sin(\alpha-\beta)}{h_a}\right].$$

but as far as:

(36)
$$G_{\xi}=\frac{f}{\delta_0}\left[\cos\alpha-\frac{dh_a}{d\alpha}.\frac{\sin\alpha}{h_a}\right].$$

(37) $$G_\eta = \frac{f}{\delta_0}\left[\sin\alpha - \frac{dh_a}{d\alpha}.\frac{\cos\alpha}{h_a}\right].$$

Then: (38) $$G = G_\xi \cos\beta + G_\eta \sin\beta$$

At a circular diagram $\frac{dh_a}{d\alpha} = 0$ and then:

(39) $$G = \frac{f}{\delta_0}\cos(\alpha - \beta).$$

When using the deduced ratios should be taken into account that they are effective for rapidly developing processes with small angular deviations. During Application of shift diaphragms in the apparatus allows obtaining of maximum amount of information about the experiment, and in the reverse case at the wrong choice of aperture size can be missed many details from studied process.

SATELLITE SPECTROPHOTOMETER FOR MONITORING OF THE ATMOSPHERE

The spectrophotometer is designed for research of the spectral and energetic characteristics of the atmosphere, in particular ozone, sulfur dioxide and other gases (Fig. 11).

The spectrophotometer for atmosphere research consists of a step motor 1, which via a kinematic unit 2 is connected with two mechanical axes 3 and 4. To the axis 3 is mounted a reflective element 11 and to the shaft 4 - reflective element 21. The two reflective elements 11 and 21 are connected in such a way that during their scanning movement their reflection planes remain mutually parallel.

In front of the reflective elements there are two dimming (antireflective) blends, respectively 12 and 22, through which passes the radiation from the researched object 51.

On the optical axis of the reflective element 11 are arranged alternately lens 13 and optical coupler 14, mechanically connected to the step motor 15 controlled by microprocessor system 50. On the one outlet of the optical coupler 14 is mounted the start of the lightguide 16, and to the other outlet is mounted a photoreceiver 17, whose outlet is electrically connected to the unit for signal processing 18, and the outlet of unit 18 is connected to the microprocessor system 50. Units 11, 12, 13, 14, 15, 16, 17 and 18 form the photometric tract 10 of the spectrophotometer. In a similar manner to the optical axis starting from the reflective element 21, part of the said spectrometric tract 20, are placed in succession lens 23 and optical coupler 24, mechanically connected to the step motor 25, also electrically connected to the microprocessor system 50. One input of the optical coupler 24 is connected to the optical lens 23, into the second

input is connected the end of the light guide 16, the third input via light guide 26 is connected to the photo converter 27, and the fourth is connected via light guide 28 with a reference source 29. At the output of the optical coupler 24 is placed inlet diaphragm 30 mechanically connected via reducer 31 to the step motor 32, which is electrically connected to the microprocessor system 50. On the optical axis from the output of the optical coupler 24, passing through the aperture 30 is positioned a concave diffraction grating 33, mechanically connected via reducer 34 to the step motor 35, electrically connected to the microprocessor system 50. On the axis of the motor, between him and the reducer 34 is mounted the stationary converter "angle-code" 36, whose outlet is also connected to the microprocessor system 50. Opposite to the concave diffraction grating 33 is positioned Rowland circle 37 and behind its outlet slits are positioned photoreceivers 38 ', 38 ", 38"' ... 38n, which outlets are electrically connected respectively with the signal processing blocks 39 '39 ", 39 "' ... 39n, whose outlets are connected to inlets of the multiplexer 40. The outlet of the multiplexer 40 is electrically connected to the microprocessor system 50. To signal processing blocks 39 ', 39 ", 39"' ... 39n is connected an attenuator - range switch 41. In front of the photo transducer 27 is positioned tracking system 42, directed towards the Sun and mechanically connected to the converter "angle-code" 43, whose outlet is electrically connected to the microprocessor system 50. Blocks 21 to 41 form the spectrometric tract 20 of the spectrophotometer.

Operation of the spectrophotometer comprises of the following steps: the light flow emitted or reflected by the research object 51 passes through dimming apertures 12 and 22 respectively and falls onto the reflective elements 11 and 21 of the scanning system. The purpose of dimming blends 12 and 22 is to protect the lenses 13 and 23 of side illumination. Scanning reflective elements 11 and 21, put in motion by step motor 1 via kinematic block 2 and mechanical axes 3 and 4, scan the object according to a certain law, preset and controlled by the microprocessor system 50. Light signals reflected by the reflective elements 11 and 21, fall on lenses 13 and 23 respectively and after corresponding transformation enter the inlets of the optical couplers 14 and 24. The optical coupler 14 allows the input optical signal to pass directly to the photoreceiver 27 or deflect at an angle of 90° and via lightguide 16 to enter one of the inlets of the optical coupler 24. The latter allows consecutive passing of light flows from the lens 23, the internal calibration reference source 29, from the optical converter 27 and from the lightguide 16. From the outlet of the optical coupler 24 the optical signals pass through a inlet diaphragm 30 of the dispersing system. After the dispersion of the signal from the diffraction grating 33, monochromatic light flows enter through corresponding outlet slits of the Rowland Circle 37 on the relevant photoreceivers 38', 38", 38"' ... 38n-1, 38n. The photoreceivers from 38' to 38n-1 operate in mode of “parallel scan” and the

photoreceiver 38n operates in one of the modes “calibration” or “consecutive scan”. Electrical signals from the photoreceivers 38' to 38n, processed by the signal processing blocks 39', 39", 39"' ... 39n, via the multiplexer 40 enter the microprocessor system 50. The enhancement factor in the signal processing blocks 39', 39", 39"' ... 39n is regulated by an attenuator- range switch 41 controlled by microprocessor system 50.

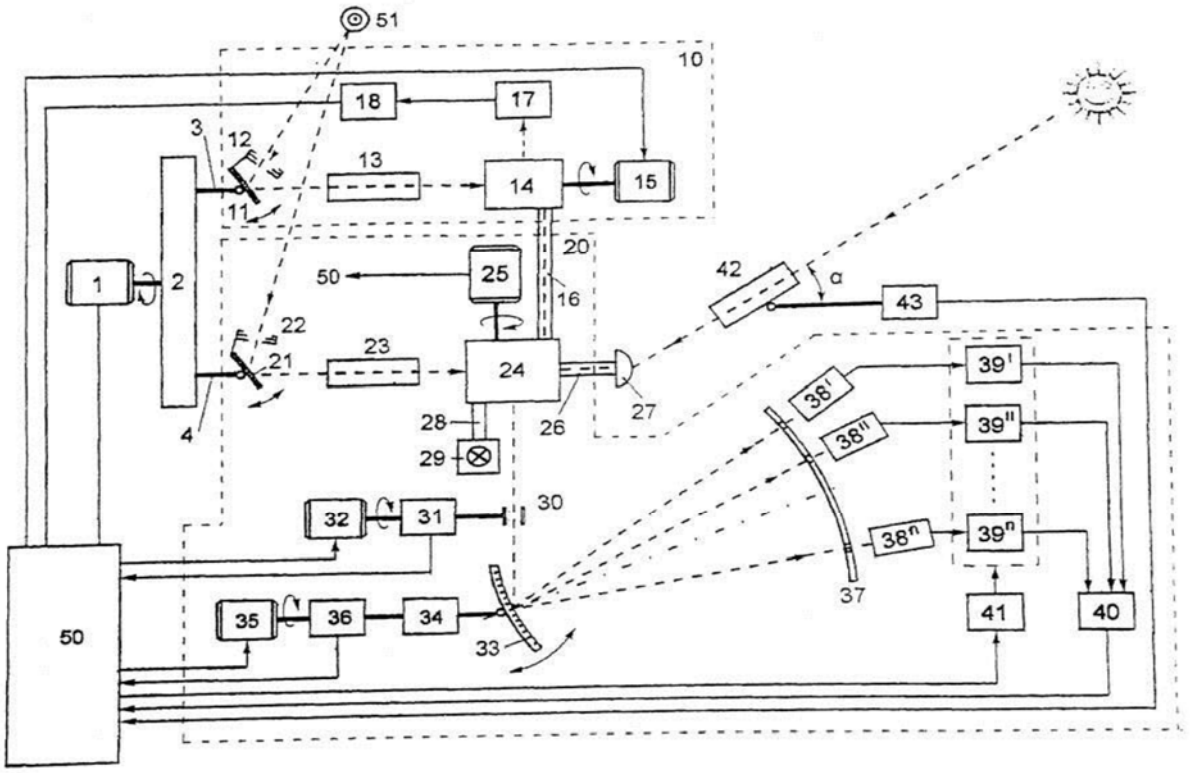

Fig. 11. A spectrophotometer for monitoring of the atmosphere

Tracking system 42 performs continuous monitoring of the center of the solar disk, so the calibration signal enters the optical converter 27.

Reflecting the height of the sun is performed by the converter “angle - code” 43 connected to the microprocessor system 50. Here is performed the information processing.

Fig. 12. Satellite laboratory spectrophotometer

SATELLITE SPECTROPHOTOMETER FOR ENVIRONMENTAL MONITORING

I. Technical field

The invention relates to a spectrophotometer for monitoring of the environment. Its application is in satellite remote methods for environmental research.

II. Background of invention

There are spectrophotometers for testing of the characteristics of gases in the atmosphere, consisting of inlet lens, entrance diaphragm, a diffraction grating driven by a step motor, an outlet diaphragm, photo detectors and electronic amplifier. Such spectrophotometer operates on the principle of consecutive scanning (based on dispersive diffraction grating).

It is also known a multispectral equipment “Fragment”, designed to operate aboard the space crafts on Earth orbit, which contains scanning system, lens, optical splitter, spectral filters, amplifier and a system for signal processing.

The disadvantage of these known devices are the low spatial resolution, limited spectral area of research, poor accuracy, poor reliability, slow performance and poor repeatability of the results on calibration.

It is also known the equipment mounted on satellites "IUE", consisting of inlet lens, dispersion system and recorder. The disadvantage of this equipment is the low reliability and poor accuracy.

It is also known an ozone spectrometer consisting of an optical system, diffraction grating, a system of outlet diaphragms and calibrating device. A disadvantage of this spectrometer is its poor functionality.

Existing devices are not able to photograph the research object, which significantly decreases the effectiveness of research.

III. Object of invention

The object of invention is to provide a satellite spectrophotometer for monitoring a of the environment, without those drawbacks.

IV. Thecnical summary of the invention

The problem is solved by inventing of a satellite spectrophotometer for environmental monitoring, consisting of spectral and photometric tract and channel for transmitting of a satellite image.

The advantages of the invention are improved accuracy, smaller weight, overall dimensions and energy consumption, increased spatial and temporal resolution, speed, better reliability and increased volume of useful information.

V. Description of the drawings

An example embodiment of the invention is shown in Figure 1, showing the block diagram of a satellite spectrophotometer for environmental monitoring.

VI. Example of an embodiment of the invention

As shown on Figure 1, the satellite spectrophotometer for environmental monitoring consists of dimming aperture 1, located in front of a flat scanning mirror 2 with fitted to it reference source 3, related to both photometric and spectrometric channel and representing the input scanning system controlled by a step motor 22. The step motor 22 is connected mechanically via gear drive 23 to the scanning mirror 2 and electrically to the photoelectric converter angle - code 24 for carrying out of a feedback. Opposite to the scanning flat mirror 2 on

the same optical axis is located concave mirror 5, and between them is mounted fixed prism 4 which guides one fraction of the optical signal to the spectrometric, and another - to the photometric tract of the spectrophotometer. Concave mirror 5 from the spectrometric tract is optically connected to a flat mirror 6, which in turn - via inlet diaphragm 7 and through the concave mirror 8 - to a diffraction grating 9, mounted on a moving carriage 10 and then trough a camera lens 11 and an outlet diaphragm 12 to sensor 13.

Reflecting prism 4 is optically connected also with the photometric tract, that is trough the flat mirror 14, lens 15, interference filter 16 and optical lens 17 to the sensor 18. The sensors 13 and 18 parts respectively of the spectrometric and photometric tract, are connected to microprocessor system (MPS) 19 through an analog-to-digital converters (ADCs) 20 and 21.

The step motor 25 via a mechanical block 26 is mechanically connected to the carrier 10 of the diffraction grating 9, and the photoelectric converter angle- code 27 is electrically connected to the motor 25. The camera 28 is connected to the microprocessor system 19.

VII. Operation of the satellite spectrophotometer

The flat scanning mirror 2, driven by the step motor 22 and the gear drive 23 performs scan at angle $\beta = \pm 45°$, which is regulated by feedback performed by photoelectric converter angle - code 24. The optical signal reflected by the concave mirror 5 and the flat mirror 6 through the inlet diaphragm 7 falls on the concave mirror 8 and a parallel beam is passed to the diffraction grating 9, mounted on the carrier 10. The monochromatic signal from the diffraction grating 9 passes through the camera lens 11 and the outlet diaphragm 12 onto a sensor 13. The electrical signal from the outlet of the sensor 13 is digitized in the ADC 20 and submitted as an 8-digit binary code for processing in the MPS 19. The smooth scanning of the diffraction grating 9, mounted on the movable carriage 10, is performed by a mechanical block 26, coupled to the step motor 25, while the feedback for the position of the diffraction grating 9 is provided via the photoelectric converter angle-code 27.

Part of the optical signal from the reflective prism 4 enters in the photometric channel and reflected by the flat mirror 14 falls through the lens 15 on the interference filter 16. From there the monochromatic optical signal is focused through the lens 17 on the sensor 18. The resulting electrical signal is passed to the ADC 21 and in the form of an 8-digit binary code enters into the MPS 19.

The internal calibration of the spectrometric and photometric tract is performed at a closed dimming aperture 2 and the reference signal from the calibration refference source 3 is recorded as a minimum threshold sensitivity of the apparatus. The external calibration of the spectrophotometer is performed

by rotating of the inlet scanning system on 180° to the basic position (0°), i.e. in the direction of the solar disk. The functional scheme allows the researched spectral range to be scanned continuously or discretely without changing the mode of operation of the diffraction grating 9, by selective permission of passing of electrical signals as a function of the current angular position, recorded by the photoelectric converter angle - code 27. The measurement process and the registration are completely automated. The optical signal from the reflective prism 4 flows through the semitransparent flat mirror 14 to the lens of a video camera 28. Once the microprocessor system 19 detects information signal over a certain level, signal is passed to the camera 28 and is videorecorded a particular process, a phenomenon with "extreme" physical characteristics. Camcorder 28 provides perception of an image in the visible part of the optical spectrum. At a reduced illumination of the background and darkness an option is provided through electronic optical converter - amplifier the brightness of the image (module converting the infrared radiation from the object into visible) to obtain video information from the studied objects, processes and phenomena.

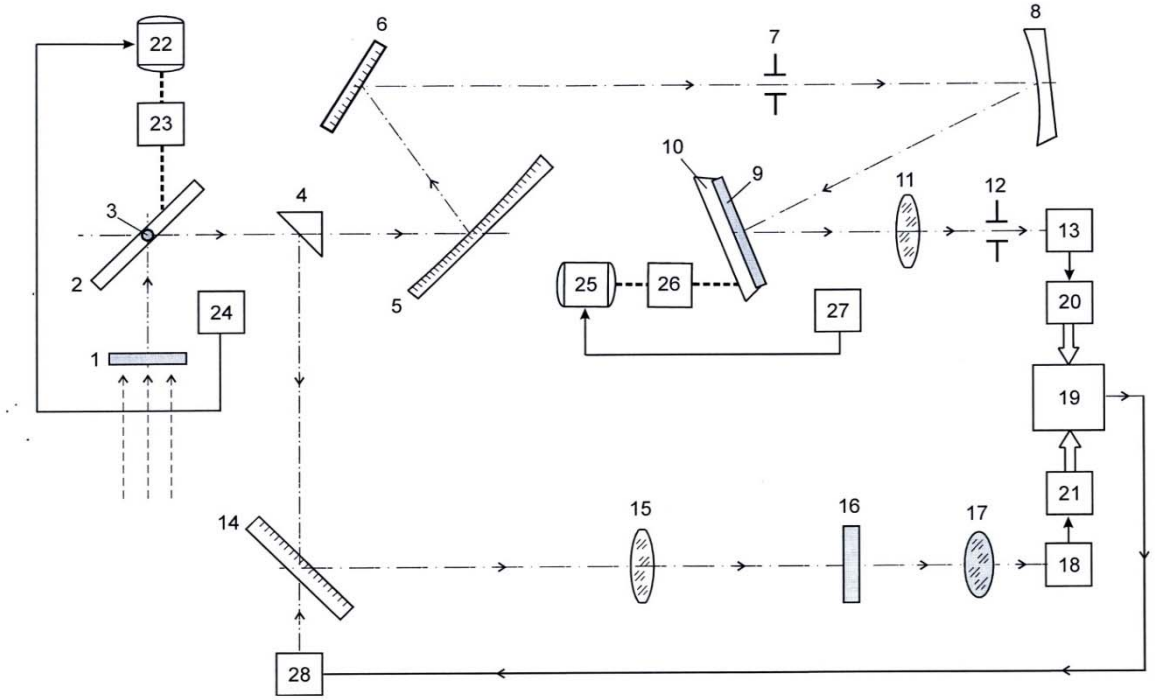

Fig. 13. Satellite spectrophotometer for monitoring of the environment

PATENT CLAIMS

Satellite spectrophotometer for environmental monitoring consisting of dimming aperture 1, flat scanning mirror 2, reference source 3, reflective prism 4, concave mirrors 5 and 8, flat mirrors 6 and 14, inlet diaphragm 7, diffraction grating 9, lens 11 and 15, outlet diaphragm 12, sensors 13 and 18, interference

filter 16, optical lens 17, microprocessor system 19, analog-to-digital converters (ADCs) 20 and 21, step motors 22 and 25, gear drive 23, photoelectric converters angle-code 24 and 27, mechanical block 26, where the dimming aperture (1) is positioned in front of the flat scanning mirror (2) with mounted in it reference source (3), which constitute an input scanning system of photometric and the spectrometric tract and are mechanically coupled to the step motor (22) via the gear (23). The photoelectric converter angle-code (24) is electrically connected to the step motor (22) and opposite to the flat scanning mirror (2) on the same optical axis is positioned concave mirror (5) and between them is fixed the reflecting prism (4), optically connected to the concave mirror (5) of the spectrometric tract, and to the flat mirror (14) of the photometric tract. The concave mirror (5) is connected optically with the flat mirror (6), which in turn through the inlet diaphragm (7) has an optical connection to the concave mirror (8) and from there to a diffraction grating (9) mounted on a movable carrier (10). The diffraction grating (9) is connected optically through the lens (11) and the outlet diaphragm (12) to the sensor (13). The flat mirror (14) of the photometric tract is connected optically through the lens (15), the interference filter (16) and the optical lens (17) to the sensor (18). The sensors (13) and (18), respectively parts of the spectrometric and photometric tracts, are electrically connected to microprocessor system (MPS) (19) through the analog-digital converters (ADCs), respectively (20) and (21). The step motor (25) via a mechanical unit (26) is mechanically connected to the carrier (10) of the diffraction grating (9). The photoelectric converter angle-code (27) is electrically connected to the electric motor (25), the reflective prism (4) via the semi-transparent flat mirror (14) is optically connected to the input of the camera (28) and to same camera is connected the MPS outlet (19).

PROSPECTS FOR SATELLITE RESEARCH

Interesting experiments planned in the near future will enable to determine the amount of many TGC (O_3, H_2O, N_2O_5, N_2O, CF_4, HNO_3, CH_4, SO_2, CO, CO_2 and etc.). It is supposed substantial development of the system for atmospheric research with the use of geostationary satellites.

CONCLUSION

The analysis of the current state of satellite research for studying of the gas composition of the atmosphere has led to the following conclusions:

1. In recent years, using a variety of satellite methods, have been obtained a large amount of unique information about the content of the TGC in the Earth's atmosphere. Have been studied their spatial - temporal variations on different spatial and temporal scales, have been detected and assessed the

contents of the new TGC, has been received new information about the stratosphere dynamics.

2. The satellite system for studying of the gas composition of the atmosphere is an important part of the global system for monitoring the state of the environment, and in this regard, an important part is the task of optimum combination of land, air and aerostatic systems for research of TGC.

3. Different satellite methods and geometries of measurement have different advantages and disadvantagesand and substantially complement one another. When creating a satellite system for monitoring of TGC in order to increase its effectiveness and informativeness, it is appropriate to combine optimally different methods, considering the various requirements for detection and measurement of TGC when solving scientific and applied problems.

4. Modern developments in satellite methods for studying of the gas composition include expanding of the list of tested TGC, increasing the accuracy and altitude range, increasing the spatial resolution in measurements, complex determining the physical condition of the atmosphere. Solving these problems is related to establishing of a unique satellite equipment, precise research of the optical characteristics of the TGS, improving the physical basis of remote measurement, including the development of new tools and equipment.

5. Of great importance in creating of satellite-based systems for monitoring of TGS is the metrological equipment of measurements, an organization that needs extended laboratory and field research on the ground.

References:

[1] Zhekov Zh. Detection of Distant Objects on the Ground Surface from the Board of Aircrafts. Collection of Works Science Conference "Space, ecology, security", IKI – BAS, Varna, 2005, p.389-393.

[2] Zhekov Zh. Methods for Photometric Calculation of Optical Visirs for Discovery of Distant Objects in Various Brightness of the Background. II International Congress of Mechanic and Electronic Engineering and Marine Industry MEEMI 2005, TU, Varna 2005, p. 217.

[3] Zhekov Zh., G. Mardirossian. Study of the Impact of the Background on the Resolution and Determination of Variations in the Dark Current in Opto-electronic converters. Collection of Works Technical University of Varna, 2004, p. 483-489.

[4] Mardirossian G., Zh. Zhekov. Method for Determination of the Frequency – Contrast Characteristics of Electronic-optic systems. Aerospace Research in Bulgaria 19, 2005. Sofia. p. 56-62.

[5] Zhekov Zh. Methods for determining the amount of multi-electronic scintillations on the screen of electro-optic transformer of images. Thirteenth International Scientific and Applied Science Conference ELECTRONICS 2004 Sozopol, p. 106-110.

[6] Zhekov Zh., G. Mardirossian. Energy Efficiency of a System for Primary Processing of Signals in a Opto-Electronic Device operating under low-contrast conditions. Thirteenth International Scientific and Applied Science Conference ELECTRONICS 2004 Sozopol, p. 111-116.
[7] Zhekov, Zh., D. Ivanova, K. Valtchev. An Analysis Of The Atmospheric Transparency By A Satellite Spectral Limb Method And A Pulse, Photometric Apparatus "Terma", XXVI Colloquium Spectroscopicum Internationale. Abstracts. Vol. I, National Palaca Of Culture, Sofia, 1989, P. 221.
[8] Zhekov, Zh., G. Mardirossian, I. Hristov, D. Ivanova. Absorption Ultraviolet Ozonometer. Bulgarian Geophysical Journal, Vol. XXIV, N 3 – 4, Sofia, 1998, P. 50 – 54.
[9] Getsov, P., Zh. Zhekov, G. Mardirossian, S. Stoyanov, M. Varbanov, S. Velkoski. Total Content Of Atmospheric Ozone Measurement Apparatuses, Created In The Space Research Institute At The Bulgarian Academy Of Sciences, 2nd Congress Of Ecologist Of The Republic Of Maedonia With International Participation. Ohrid, Macedonia, 2004, P. 534 – 537.
[10] Getsov, P., Zh. Zhekov, G. Mardirossian, S. Stoyanov, M. Varbanov, S. Velkoski. Total Content Of Atmospheric Ozone Measurement Apparatuses, Created In The Space Research Institute At The Bulgarian Academy Of Sciences, 2nd Congress Of Ecologist Of The Republic Of Maedonia With International Participation. Ohrid, Macedonia, 2004, P. 534 – 537.
[11] Hristov, I., Zh. Zhekov, G. Mardirossian, D. Ivanova. Satellite. Absorption. Ozonometer. Aerospace Research In Bulgaria, N 15, 1999, P. 27 – 32.
[12] Hristov, I., Zh. Zhekov, T. Stantchev. An Analysis Of Constructional Solutions About Dispersing System With A Mobile Diffraction Lattice. XXVI Colloquium Spectroscopicum Internationale. Abstracts. Vol. I, National Palace of Culture, Sofia, 1989, P. 221.
[13] Zhekov, Zh . Methods for Dethermining the Amount of Multi-electronic Scintillations on the Screen of Electro – optic Transformer of Images. Journal SCIENTIFIC AND APPLIED RESEARCH, Vol 3, 2013, p 68 – 73.
[14] Zhekov, Zh. , G. Mardirossian. Influence of the Transmission Processes Upon the Background Bringhtness and Relation Between the Dark and Background Scintillations of Electro – optic Transformer. Journal SCIENTIFIC AND APPLIED RESEARCH, Vol 4, 2013, p 26 –31.